Synthesis, of some transition metal (II/III)-Schiff base complexes and copper, zinc nanoparticle size bearing sulfonamide fragment : New drugs for antimicrobial and anticancer agents.

***A. A. Salman, *Carmen M.Sharaby, ** Abdel Fatah. M. B, Fatma M.A.**

* *Chemistry Department, Faculty of Science, Al-Azhar University (Girls), Nasr City, Cairo, Egypt.*

** *Applied Chemistry, Institute Research Petroleum, Nasr City, Cairo, Egypt.*

ABSTRACT

A simple approach to the synthesis metal complexes and copper, zinc nano particles size (CuNPs, ZnNPs) of novel Schiff base of sulfonamide ligand (HL) resulted from the condensation of sulfametrole [N'-(4-methoxy-1,2,5-thiadiazol-3-yl]sulfanilamide and 1-(2-Furanyl) ethanon. The metal complexes and copper, zinc nano particles size (CuNPs, ZnNPs) of HL ligand were synthesized and characterized using different physico-chemical studies as elemental analyses, mass spectra, conductivity measurement, UV-vis Spectra, solid reflectance, IR spectra,,^{1}H NMR spectra, magnetic susceptibility, thermal analyses (TGA and DTA), (TEM) Transmission Electron Microscope and their microbial and anticancer activities . The spectroscopic data of the complexes suggest their 1:2(L:M) complex structures. Also the spectroscopic studies suggested the octahedral structure for all complexes. The size and morphology investigation of copper and zinc nano particles (CuNPs, ZnNPs) with (HL) ligand by TEM images indicate that the copper and zinc nano (CuNPs, ZnNPs) show spherical shape with core shell of HL ligand. The synthesized Schiff base and its metal complexes, CuNPs, ZnNPs were screened for their bacterial, antifungal and anticancer activity. The activity data show that the metal complexes, CuNPs and ZnNPs to be more potent than the parent HL Schiff base ligand. Also the data show that the CuNPs and ZnNPs more potent than the metal complexes and than HL free ligand .

Keywords: New Schiff base of sulfonamide, transition metal complexes, CuNPs, ZnNPs and antimicrobial, anticancer activity.

Introduction

Schiff bases are an important class of organic compounds[1.2]. They were first reported by Hugo Schiff in 1864[2].The Schiff base ligands and their corresponding metal complexes have expanded enormously and include a vast area of organometallic compounds and various aspects of bioinorganic chemistry[3]. Schiff base ligands have been reported to show a variety of biological actions by virtue of the azomethine linkage, which is responsible for various antibacterial, antifungal, herbicidal,clinical and analytical activities[4]. Transition metal complexes with oxygen and nitrogen donor Schiff bases are of particular interest[5,6], because of their ability to possess unusual configuration[3]. On the other hand, azo compounds are very important molecules and have attracted much attention in both academic and applied research [3]. Azo compounds and their metal complexes are known to be involved in a number of biological reactions, such as inhibition of DNA,RNA, and protein synthesis, nitrogen fixation, and carcinogenesis[7]. Schiff bases derived from aromatic amines and aromatic aldehyde have a wide variety of applications in many fields as sulfonamide Schiff bases which

have been reported to posses-anti-microbial[8], anti-inflammatory activity[29], antikinetoplastid antimitotic activity[29], antitumor activity and anticonvulsant activity[9].The present work was devoted to elucidating the structures of new series of Fe(III), Fe(II), Cu(II), Zn(II), Cd(II), Ce(III), UO_2(II) complexes and copper, zinc metal nanoparticles (CuNps,ZnNps) with HL Schiff base ligand 4-(1-Furan-2-yl-ethylideneamino)-N-(4-methoxy-1,2,5- thiadiazol-3-yl)-benzenesulfonamide and to check their biological activities[2].

Nanocomposites are composites in which at least one of the phases shows dimensions in the nanometre range (1nm = 10^{-9}m)[10]. Nanocomposite materials have emerged as suitable alternatives to overcome limitations of microcomposites and monolithics, while posing preparation challenges related to the control of elemental composition and stoichiometry in the nanocluster phase. They are reported to be the materials of 21st century in the view of possessing design uniqueness and property combinations that are not found in conventional composites[10]. The general understanding of these properties is yet to be reached, even though the first inference on them was reported as early as 1992[10].

2. Experimental

2.1. Materials and reagents

All chemicals used were of the analytical reagent grade(AR), and of highest purity available. Sulphametrole, 1-(2-furanyl)-ethanone and ferric chloride hexahydrate ($FeC1_3.6H_2O$), ferrous sulphate heptahydrate ($FeSO_4.7H_2O$), copper chloride dihydrate($CuC1_2.2H_2O$), zinc chloride anhydrous($ZnC1_2$), cadmium chloride monohydrate($CdC1_2.H_2O$), cerum chloride anhydrous ($CeCl_3$) and uranyl nitrate anhydrous $UO_2(NO_3)_2$ and copper, zinc metal nano particles (CuNps,ZnNps) were purchased from (B.D.H Merck, Sigma or Fluka) and the organic solvents (ethanol, diethylether, deutrated dimethylsulfoxide (DMSO), and dimethyl formamide (DMF), were purchased from BDH. Perchloric acid, ammonium nitrate, ammonia solution, ammonium chloride, nitric acid, potassium dichromate and ethylenediamintetraacetic acid disodium salt (EDTA) were BDH or Merck products. Murexide, Eriochrom black-T(EBT) were used as indicators BDH or Merck products. De-ionized water collected from all glass equipments was usually used in all preparations.

2.2. Instrumentation

The molar conductance measurements of complexes were carried out in DMF (10^{-3}M) using a Jenway 4510 conductivity meter. Elemental analyses of the separated solids for C, H, N, S and Cl were performed at the Microanalytical Center,Cairo University, Giza, Egygpt. The UV-vis absorption spectra and solid reflectance were measured at room temperature in UV-vis range(200-800nm) using Shimadzu PC 3101 UV-vis spectrophotometer, at the Regina Center for Mycology Biotechnology, Al-azhar University , Cairo, Egypt.Infrared spectra were recorded, as KBr pellets, on a Perkin–Elmer FT-IR type 1650 spectrophotometer in wave number region 4000–400cm^{-1}. ^{1}H NMR spectra (DMSO-*d6*) were recorded with Bruker FT-400MHZ spectrometer. Chemical shift for proton resonances were reported in ppm(δ) relative to tetramethylsilane(TMS).The molar magnetic susceptibility was measured on powdered samples using the Faraday method. The diamagnetic corrections were made by Pascal's constant and $Hg[Co(SCN)_4]$ was used as a calibrant. Thermal analyses (TGA and DTA) the prepared complexes were carried out in dynamic nitrogen atmosphere (20mL min^{-1}) with heating rate of 10°Cmin^{-1} using Shimadzu TGA-50H and DTA-50H at Cairo University, Egypt. The percent weight loss was measured from ambient temperature up to 1000°C, where highly sintered α-Al_20_3 was used as a reference. Transmission electron microscopy (TEM) images were obtained by using a Jeol 2010 named DV 300W1 system operating at 130 kV. TEM images were used to determine the partical size.

2.3. Synthesis of Schiff base (HL)

Schiff base ligand HL was prepared by mixing hot ethanolic solution (≈60°C)

of the ketone, 1-(2-furanyl)-ethanone (5.46g, 0.05mmol) to hot ethanolic solution (≈60°C) of sulphametrole, [N\-(4-methoxy-1, 2, 5 - thiadiazole-3-yl) sulfanil-amide] (14.361g, 0.05mmol) in 50ml quickfit flask. The reaction mixture was heated under reflux for ≈3hr under anhydrous conditions with continuous stirring and the formed solid product was separated by filtration, purified by crystallization from ethanol, washed with diethyl ether and dried in vacuum over anhydrous calcium chloride. The yield of brown crystals of HL was 94% with m.p=180°C.

2.4. Synthesis of metal complexes

The metal complexes of HL ligand were prepared in 1:2 (L:M) molar ratio.The complexes were prepared by the addition 25ml hot ethanolic solution (≈60°C) of metal chloride or nitrate or sulphate (2mmol) to 25ml hot ethanolic solution (≈60°C) of Schiff base (1mmol).The resulting mixture was stirred under reflux for ≈2 hr where upon the colored complexes precipitated. They were separated by filtration, purified by crystallization from ethanol, washed several times with diethyl ether and dried under vacuo.

2.5.Synthesis of copper or zinc metals nanocomposites (CuNPs, ZnNPs).

The nanocomposite were prepared by addition 2g of copper or zinc nano-particles (CuNps,ZnNps) were dissolved to (10ml) in N,N-dimethyl formamide (DMF) and then were slowly mixed with 1g of Schiff-base(HL) dissolved to (10ml) in N,N-dimethyl formamide (DMF). The mixture was stirred for 24h at room temperature and then dried under vacuum. After the removal of DMF, the nanoparticle composites were formed .The composites were washed several times with DMF and diethyl ether and almost no free Schiff-base could be found in the solution, indicating that almost all of ligand (HL) has been combined with the copper or zinc nanoparticle and the content of copper or zinc metals in Schiff-base was 66.66%.

2.6. Biological activity

This paper aims to the discovery of new metal complexes and nanoparticle composite compounds against new target which is a matter of urgency. So the antimicrobial and antitumor activity of the new synthesized free Schiff base ligand HL and its metal complexes and nanoparticle composites were studied.

The free Schiff-base ligand (HL) and its metal complexes and nanoparticle composites were screened against micro-organism,Gram positive(+ve) bacteria; *Staphylococcus aureus (ATCC 25923)* and *Bacillus subtilis(ATCC 6635)*, Gram negative(-ve) bacteria *Salmonella typhi-murium (ATCC 14028)* and Escherichia coli *(ATCC 25922)*, Yeast; *Candida albicans (ATCC 10231)* and fungi; *Aspergillus fumi-gatus* to assess their potential antibacterial and antifungal activities. The antibiotic, Chloramphenicol and Cephalothin were used as standard antibacterial control and Cyloheximide as standard Yeasts and Fungi control using agar mutrient as the medium. The test solutions of two concentrations, 1mg/L and 0.5mg/L were prepared by dissolving the newly synthized compounds in DMF as a solvent, then poured on agar medium with microorganisms. At 35^{0}C for 24 hr during this time the tested solution diffused and the growth of inoculated microorganisms were affected. The inhibition zone appear on the plate was measured[(1)]. The action of the free HL ligand and that its metal complexes against bacterial, Yeasts and Fungal species were recorded in **Tables 8,9.** The in-vitro anticancer activity evaluation of the newly synthesized compounds HLligand and their metal complexes and nanocomposites was carried out against human cancer cell line (HCT-116) (human colon cancer cell lien).

3. Results and discussion

3.1. Schiff base characterization

The new prepared HL Schiff-base ligand, 4-(1-Furan-2-yl-ethylideneamino)-N- (4methoxy-[1,2,5]thiadiazol-3-yl) benzen sulfonamide was subjected to elemental analyses, mass spectra, IR and ^{1}H NMR spectral studies. The results of elemental analyses (C, H, N, S and Cl) and the

suggested molecular formula of HL ($C_{15}H_{14}N_4O_4S_2$) and **Table 1** are shown in **Figure 1.** The melting point are presented in **Table 1**. The melting point of HL Schiff base ligand is sharp indicating the purity of this new prepared ligand. The mass spectra **Figure 2**, **Schem 1** show the mole- cular ion peak at m/z= 378(3%), which compatible with molecular formula $C_{15}H_{14}N_4O_4S_2$ of HL Schiff base ligand. The base peak appeared at m/z=77(100%) was recorded to HL ligand. The other mass fragmentation patterns are shown in **Figure 2**, **Schem 1** . The UV-vis spectrum of HL Schiff base ligand was recorded in (10^{-3}M) DMF as solvent. The spectrum show the characteristic absorption bands at λ_{max}=284nm, λ_{max}=368nm which can by assigned to π-π^* and n-π^*transitions respectively for HL Schiff base ligand[11,12], **Table 4**. The IR spectral data, **Table 2** in the region 4000-400cm^{-1} have been recorded for the HL Schiff base ligand. The IR data show that the υ(CH=N) of the azomethine group and υ(C=N) of the thiadiazole moiety occur at 1596cm^{-1} and 1629cm^{-1}, respectively[13-15]. In addition, the ligand exhibits two bands at 1330 and 1130cm^{-1} which is attributed to $\upsilon(SO_2)_{asym}$ and $\upsilon(SO_2)_{sym}$ stretching vibrations,respectively[16,17]. Also, it has a band at3452cm^{-1} which attributed to υ(NH)[12]. The ^{1}H NMR data for HL Schiff base ligand, **Table 5,** are recorded in DMSO-*d6*[18-20], which show sharp signals at 2.59 and 3.94 ppm which may be assigned to the (-CH_3=N,3H)and (-OCH3; 3H) protons[21,22], respectively. Another doublet–doublet band observed at 7.54-7.59ppm for HL Schiff base ligand assigned to the p-di substituted benzene ring [23,24]. The broad band observed at 11.25ppm may be attributed to the secondary amine proton (-SO_2-NH;1H) (exchangeable with D_2O)[20,22].

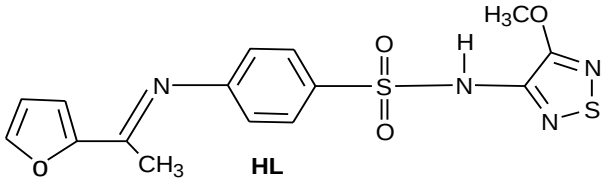

HL

Fig.1. suggested structure of newly synthesized HL Schiff base ligand.

Table 1. Elemental analyses and some physical measurements of HL Schiff base ligand and its metal complexes **(1-7).**

Compd. No. Emprical formula	M.P. (°C)	Color (Yield %)	(%) found (Calcd.)						*Λm* Ω^{-1}mol^{-1}cm^2
			C	H	N	S	CL	M	
HL $C_{15}H_{14}N_4O_4S_2$. 378	180	Brown (94)	47.61 (47.35)	3.70 (3.92)	14.80 (14.5)	16.90 (17.1)	_	_	9.66
(1)[$(FeCl_3)_2$(HL)$(H_2O)_2$].H_2O $C_{15}H_{24}Cl_6Fe_2N_6O_9S_2$. 734	>300	Dark green (72)	24.37 (24.15)	1.89 (1.45)	7.58 (7.80)	8.66 (8.11)	29.23 (29.01)	15.10 (15.80)	28.58
(2)[$(FeSO_4)_2$(HL)$(H_2O)_4$].H_2O $C_{15}H_{24}Fe_2N_6O_{17}S_4$. 771.60	>300	Coffe (77.20)	23.88 (23.90)	1.85 (1.64)	7.43 (7.62)	8.49 (8.24)	_	14.80 (15.30)	20.21
(3)[$(CuCl_2)_2$(HL)$(H_2O)_4$].H_2O $C_{15}H_{24}Cl_4Cu_2N_4O_9S_2$. 736	>300	Dark brown (90.80)	25.03 (25.64)	1.94 (1.55)	7.78 (7.92)	8.90 (9.11)	19.36 (19.29)	17.61 (18.10)	21.57
(4)[$(ZnCl_2)_2$(HL)$(H_2O)_4$]·H_2O $C_{15}H_{24}Cl_4N_6O_9S_2Zn_2$. 640.8	>300	Faint brown (85.40)	24.90 (24.42)	1.93 (1.74)	7.74 (7.70)	8.90 (9.11)	22.07 (22.15)	17.58 (17.99)	25.90
(5)[$(CdCl_2)_2$(HL)$(H_2O)_4$].H_2O $C_{15}H_{24}Cd_2Cl_4N_6O_9S_2$. 834	>300	Faint coffe (96)	22.03 (22.41)	1.71 (1.82)	6.85 (6.34)	8.85 (8.92)	17.32 (17.02)	17.51 (17.92)	19.00
(6)[$(CeCl_3)_2$(HL)$(H_2O)_2$].H_2O $C_{15}H_{24}Ce_2Cl_6N_6O_9S_2$. 820.70	>300	Faint brown (70.90)	19.84 (19.52)	1.54 (1.32)	6.17 (6.47)	7.83 (7.91)	_	_	11.85
(7) [$(UO_2)_2$(HL)$(NO_3)_4$].H_2O $C_{15}H_{15}N_8O_{21}S_2U_2$. 118	>300	Brown (71)	15.45 (15.83)	1.28 (1.26)	9.57 (9.54)	28.66 (28.37)	_	_	18.73

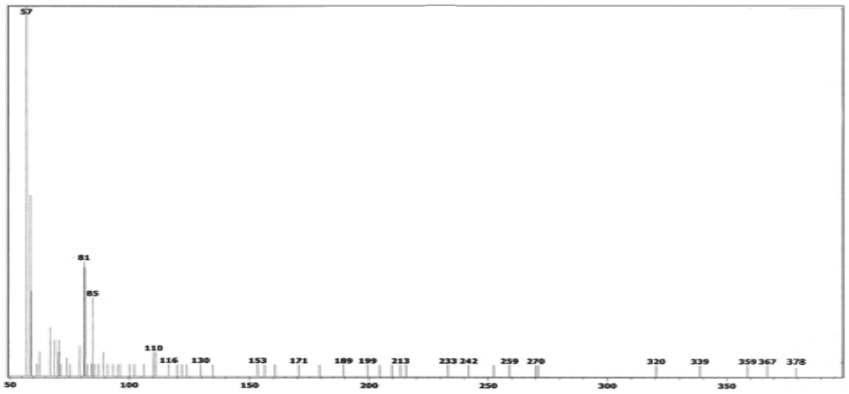

Fig.2. Mass spectrum for HL Schiff base ligand.

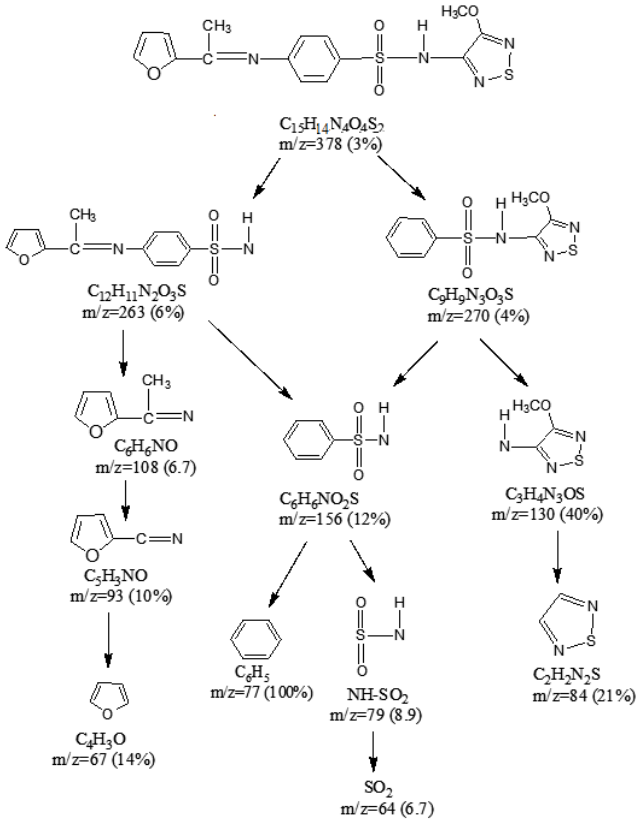

Scheme 1. Mass fragmentation pattern of HL Schiff base free ligand.

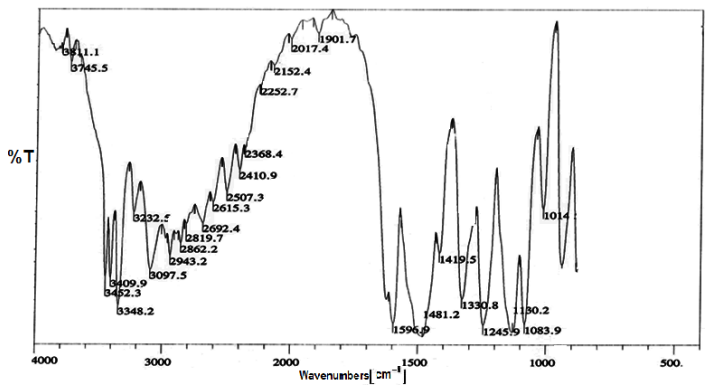

Fig.3 . IR spectrum for HL Schiff-base ligand.

Table 2. IR spectra (4000-500 cm^{-1}) of the HL Schiff base ligand and its metal complexes **(1 -7).**

Complexes.Compd. No.	υ (NH)	υ (OH) enolic	υ (SO_2) (asym.)	υ (SO_2) (sym.)	υ (C=N) thiodiaza.	υ (CH=N) azomethine	υ (H_2O) (Coord / Lattic.)	υ (M-O)	υ (M-N)
HL	3452br	--	1330br	1130sh	1629br	1596sh	--	--	--
(1)$[(FeCl_3)_2(HL)(H_2O)_2]\cdot H_2O$	--	3336br	1312m	1165br	1616sh	1595w	825br	542w	472w
(2)$[(FeSO_4)_2(HL)(H_2O)_4]\cdot H_2O$	--	3332sh	1325sh	1153br	1600sh	1512w	887m	543sh	466w
(3)$[(CuCl_2)_2(HL)(H_2O)_4]\cdot H_2O$	--	3363w	1315sh	1153sh	1622sh	1522m	891m	551m	443w
(4)$[(ZnCl_2)_2(HL)(H_2O)_4]\cdot H_2O$	--	3336br	1327w	1153m	1618w	1553 w	837m	543w	422m
(5)$[(CdCl_2)_2(HL)(H_2O)_4]\cdot H_2O$	--	3332sh	1326sh	1153sh	1622m	1593 m	887sh	543sh	462br
(6)$[(CeCl_3)_2(HL)(H_2O)_2]\cdot H_2O$	--	3325w	1326sh	1155sh	1627m	1597sh	883br	545m	435sh
(7) $[(UO_2)_2(HL)(NO_3)_4]\cdot H_2O$	--	3375w	1315br	1161sh	1627br	1515 m	833m	543m	462br

sh=sharp, m=medium, w=weak

Table 3. ^1H NMR data for HL Schiff base ligand and their diamagnetic complexes **(4, 5,7).**

	Chemical Shift (δ in ppm)						
Complexes.Compd. No.	Aromatic protons	-SO_2NH protons	-CH heterocyclic protons	Coordinate water protons	-OCH_3 protons	-OH enolic protons	-CH_3 C=N protons
HL	7.54-7.57 (d, 4H)	11.25 (br, H)	6.50 (s, H)	_	3.94 (s, 3H)	_	2.59 (br, 3H)
(4)$[(ZnCl_2)_2(HL)(H_2O)_4]\cdot H_2O$	7.56-7.59 (d, 4H)	_	6.54 (s, H)	3.43 (br, 8H)	3.98 (s, 3H)	6.00 (br, H)	2.50 (br, 3H)
(5)$[(CdCl_2)_2(HL)(H_2O)_4]\cdot H_2O$	7.55-7.58 (d, 4H)	–	6.53 (s, H)	3.42 (br, 8H)	3.98 (s, 3H)	6.00 (br, H)	2.50 (br, 3H)
(7) $[(UO_2)_2(HL)(NO_3)_4]\cdot H_2O$	7.56-7.59 (d, 4H)	–	6.54 (s, H)	3.43 (br, 8H)	3.98 (S, 3H)	6.98 (br, H)	2.50 (br, 3H)

s=singlet, d=doublet, br=broad

3.2. Composition and structure of Schiff base complexes

The isolated solid complexes of Fe(III),Fe(II),Cu(II),Zn(II),Cd(II),Ce(III) and UO_2(II) ions with the HL Schiff base ligand were subjected to elemental analyses (C, H, N, S and Cl), IR,^1H NMR, molar conductance, magnetic studies, thermal analyses (TG and DTA) and Transmission electron microscopy (TEM), to identify their tentative formulae in a trial to elucidate their molecular structures. The results of elemental analyses, **Table 1**, are in good agreement with those required by the proposed formulae **Fig. 4**. The complexes are insoluble in water and most organic solvents and soluble in DMF and DMSO solvents.

3.3. Molar conductunce measurements

By using the relation Λ_m= K/C, the molar conductance of the complexes can be calculated. The metal (II/III) complexes were dissolved in DMF (10^{-3}M) .**Table 1** shows the molar conductance values of the metal complexes which lie in the range 9-28 ohm^{-1} $mo1^{-1}Cm^2$ which indicate the non-ionic nature of metal complexes[25]. Furthermore, it indicates the bonding of the chloride or nitrate or sulphate ions to metal cations[26].

3.4. IR spectral studies

A careful comparison of the IR spectra of the metal complexes **(1-7)** and their parent Schiff base ligand(HL) was listed in **Table 2** and shown in **Fig. 3**. It

reveals that the spectra of the complexes**(1-7)** shows absorption bands of the sulphone group of $\upsilon_{asym}(SO_2)$ and $\upsilon_{sym}(SO_2)$ shifted to lower frequency than its parent HL ligand at 1327-1312cm^{-1} and at 1153-1165cm^{-1} respectively[14,27].

On the other hand the υ(NH) group disappear in the spectra of the complexes, the disappearance of this υ(NH) and the shift of SO_2 stretching vibration bands to lower frequencies attributed to the enolization of the sulfonamide (-SO_2NH) group to the enol form (-SO(OH)=N) as a result of complexation to give more stable six-memberedring[28,29]. This transformation would results in the appearance of a new absorption peak of enolic υ(OH) stretching mode at 3375-3325cm^{-1} for HL Schiff-base metal complexes[30].

The lower frequencies of the new enolic OH group shown in the metal complexes **Table 2,** which indicates the contribution of this group in the coordination[19]. Also the new bands observed at 891-825cm^{-1} in spectra of metal complexes were attributed to the stretching and out of plane bending vibrations of coordinated water molecules[31,32]. This coordinated water molecules were ducted using the thermal gravimetric analyses studies.

The azomethine υ(CH=N) group was shifted to lower wavenumbers in the spectra of the complexes due to the contribution of this group in the coordination [33]. However, the band due to the thiadizole moiety; υ(C=N) was shifted to lower frequencies at 1627-1600cm^{-1} in the spectra of the complexes, suggesting the coordination via thiadiazole nitrogen [34,35] .

Also the IR spectra of the metal complexes show two additional of bands at 551-542cm^{-1} and at 472-435cm^{-1} assigned to υ(M-O) and υ(M-N) stretching vibrations respectively [33,34] .

3.5. ^{1}H NMR spectra

The proton magnetic resonance for the diamagnetic metal complexes(4,5,7) were recorded in DMSO-d_6[16,19,20] ,**Table 3**. On comparison, the characteristic proton signals of the complexes Zn(II),Cd(II) and UO_2(II) with those of their parent HL Schiff base ligand were shown in **Table 3**. It is found that upon complexation, enolization of the secondary amine(-SO_2NH) of HL Schiff base ligand also observed and a new enolic (-S(O)(CH=N)) appeared at δ=6.00ppm, δ=6.00ppm, δ=6.98ppm for Zn(II), Cd(II) and UO_2(II) complexes respectively [18,29]. Meanwhile the laser intense signal assigned to (-CH_3C=N) proton signal observed at δ=2.50ppm δ=2.50 for Zn(II), Cd(II) and UO_2(II) complexes of HL Schiff-base ligand[21].

Furthermore the multiplate signals of the aromatic protons for diamagnetic complexes appeared around δ=7.54-7.59ppm [23,36,37].

From the above it camcoloted that HL Shiff base ligand coordinated to the metal ions through two sites, the first one is enolic-OH of sulfonamide group and 1,2,5 thiadiazol-N and the second site azomethine-N and 1-(2-furanyl)-ethanon-O.

3.6. Electronic spectra and magnetic properties

The electronic spectra of the metal complexes displayed in (l0^{-3}M) DMF at room temperature at wavelength range from 200-800nm are shown in **Table 4**. All the complexes show two main absorption bands similar to the absorption spectrum of the HL Schiff base ligand which are shifted to lower and higher wavelengths in the regions 275-208cm^{-1},479-316cm^{-1} which assigned to π-π^* and n-π^* transitions for the metal complexes, respectively[11,12,21], **Table 4**. Also *d-d* transitions in this type of complexes appear in the region782-692cm^{-1}[27].

From The electronic spectra of complexes, **Table 5** is observed that Fe(III) complex exhibit a band at 19.249 cm^{-1} assigned to $^6A_{1g}\rightarrow{}^5T_{1g}$ transition. Also, the bands observed at 27.173cm^{-1}, 26.595cm^{-1} attributed to $^6A_{1g}\rightarrow{}^6T_{2g}$(G) and LMCT

transitions for Fe(III) complex respectively[28,34,38]. The magnetic moment value is 5.34B.M. for Fe(III) complex, **Table 5** which indicates the octahedral geometry around Fe(III) ions [18,29,36,39].

Moreover the electronic spectrum of Fe(II) complex, **Table 5** shows two bands at 17.421cm^{-1}, 23.409 cm^{-1} for Fe(II) complex, assignable to $^5T_{2g}\rightarrow{}^2E_g$ and LMCT transitions respectively [40,41]. The value of the magnetic moment of Fe(II) complex is 5.46 B.M. which taken as an evidence for the octahedral geometry around Fe(II) ion[42]. The electronic spectrum of Cu(II) complex **, Table 5** exhibit two broad and low intensity bands cantered at 17.286cm^{-1}, 27.664 cm^{-1} for the complex assigned to $^2E_g\rightarrow{}^2T_{2g}$ and LMCT transitions respectively[31,43]. Themagnetic moment measured for the Cu(II) complex is 2.38B.M. suggesting the octahedral geometry around Cu(II) ion in the complex [44]. The magnetic moment value for Ce(III) complex is 2.13B.M. which consistent with the presence of one unpaired electron[13,45]. The observation of the magnetic moment value of the Ce(III) complexe indicates the minor participation of 4f-electron in bond formation[45,46].

The other metal complexes of Zn(II), Cd(II) and UO_2(II) are diamagnetic in nature in accordance with the d^0 or d^{10} configurations. So all complexes have octahedral structures **Table 5.**

Table 4 . Electronic spectral data of HL Schiff base ligand and its metal complexes **(1-7).**

Complexes.Compd. No.	Absorption bands(nm)		
	π-π*	**n-*π****	***d-d* transition**
HL	284	368	—
(1)[$(FeCl_3)_2(HL)(H_2O)_2$].H_2O	264, 230	358, 428	692, 782
(2)[$(FeSO_4)_2(HL)(H_2O)_4$].H_2O	214	354, 479	715
(3)[$(CuCl_2)_2(HL)(H_2O)_4$].H_2O	208, 238	335, 399	728, 762
(4)[$(ZnCl_2)_2(HL)(H_2O)_4$].H_2O	274, 265, 256, 245, 218	366	—
(5)[$(CdCl_2)_2(HL)(H_2O)_4$].H_2O	231	398	—
(6)[$(CeCl_3)_2(HL)(H_2O)_2$].H_2O	275, 243, 218	316, 361	588, 718
(7)[$(UO_2)_2(HL)(NO_3)_4$].H_2O	213	336	—

Table 5 . Magnetic moment and electronic spectral data of HL metal complexes**(1-7).**

Complexes.Compd. No.	Geometry	μ_{eff} (B.M)	Band assignment	Absorption band (cm^{-1})
(1)[$(FeCl_3)_2(HL)(H_2O)_4$].H_2O	Octahedral	5.34	$^6A_{1g}\rightarrow{}^5T_{1g}$ $^6A_{1g}\rightarrow{}^6T_{2g}$(G) LMCT(L→M)	17.436, 19.249 23.174 26.595
(2)[$(FeSO_4)_2(HL)(H_2O)_4$].H_2O	Octahedral	5.46	$^5T_{2g}\rightarrow{}^2E_g$ LMCT(L→M)	17.421 23.809
(3)[$(CuCl_2)_2(HL)(H_2O)_4$].H_2O	Octahedral	2.38	$^2E_g\rightarrow{}^2T_{2g}$ LMCT(L→M)	17.286 27.664
(4)[$(ZnCl_2)_2(HL)(H_2O)_4$].H_2O	Octahedral	--	d^{10}	--
(5)[$(CdCl_2)_2(HL)(H_2O)_4$].H_2O	Octahedral	--	d^{10}	--
(6)[$(CeCl_3)_2(HL)(H_2O)_4$].H_2O	Octahedral	2.13	--	--
(7) [$(UO_2)_2(HL)(NO_3)_4$].H_2O	Octahedral	--	d^{10}	--

3.7. Thermal analyses (TGA and DTA)

The thermogravimetric analyses of the metal complexes were recorded in **Tables 6,7**. The TGA thermogram of the complex, **[$(CuCl)_2(HL)(H_2O)_4$].H_2O,**shows three decomposition steps within the temperature range 30-700°C. The first step within the temperature range 30-220°C is related to the loss of $4H_2O$ (coordination, lattice) andC_6H_6, with a found mass loss of 20.2% (calcd.20.6%); the second step with

an estimated mass loss of 34.5% (calcd.34.8%) within the temperature range 220-520°C related to the loss of the organic part C_6H_6NO and 4Cl . The third at the rang 520-700°C with an estimated mass loss of 24.7% (calcd.25.1 %) attributed to the loss of organic part $C_3H_4N_3O_2S_2$ leaving Cu_2O as a metallic residue. The overall weight loss amounts to 81.5%(calcd.28.5%).

Also, The thermal decomposition of the complex **$[(UO_2)_2(HL)(NO_3)_4].H_2O$,** undergoes thermal decomposition pattern in three steps as follows: The first step within the temperature range of 35-210^{0}C, represents to the loss of H_2O (lattice), NO_3 and C_6H_6, with a found mass loss of 12.6% (calcd. 13.3%); the second step with an estimated mass loss of 25% (calcd. 25.2%) within the temperature range 210-250°C corresponds to the loss of organic part C_6H_6NO and $4NO_3$. The third step at the 520-680°C with an estimated mass loss 16.2% (calcd.16.6 %) attributes to loss of organic part $C_3H_4N_3O_3S_2$, leaving $2UO_2^{+2}$ as a metallic residue. The overall weight loss amounts to 53.8% (calcd.55.1%).

3.7.1.Calculation of activation thermo-dynamic parameters

Activation energy(E^*), enthalpy(ΔH^*), entropy(ΔS^*) and Gibbs free energy change of the decomposition(ΔG^*) are the thermodynamic activation parameters of decomposition processes of complexes are evaluated graphically by employing the Coats-Redfern relation[47] and Horowitz–Metzger[48]. The entropy of activation (ΔS^*), enthalpy of activation(ΔH^*) and the free energy change of activation(ΔG^*) were calculated, by using Excel computer program for complexes. The data are summarized in **Table 7 .**The high values of the activation energies reflect the thermal stability of these complexes. The entropy of activation is found to have a positive values in the complexes which indicate that the decomposition reactions unspontaneous-ly[38]. From the data **Table 7**, it was found the (ΔH^*) value and its sign, is dependent on the heat of formation of the complexes and the solvent effect[42], in all cases, it is found that the(ΔH^*) are positive values, So the reaction is endothermic [49].

Table 6. Thermogravimetric results (TG) of Cu(II) and UO_2(II) complexes **(3, 7)**.

Complexes.Compd. No.	Temp range(°C)	n*	Loss in weight Estim. / (calcd.)% Mass loss	Total Mass loss	Assignment	Metallic residue
(3)$[(CuCl_2)_2(HL)(H_2O)_4].H_2O$	30-220 220-520 520-700	3	20.2(20.6) 34.5(34.8) 24.7(25.1)	81.5(82.5)	$4H_2O$ coord /lattice &C_6H_6 4CL&C_6H_6NO $C_3H_4N_3O_2S_2$	Cu_2O
(7)$[(UO_2)_2(HL)(NO_3)_4].H_2O$	35-210 210-250 250-680	3	12.6 (13.3) 25(25.2) 16.2(16.6)	53.8 (55.1)	H_2O latice &NO_3 & C_6H_6 3(NO_3) & C_6H_6NO $C_3H_4N_3O_3S_2$	$2UO_2^{+2}$

Table 7. Thermodynamic data for the thermal decomposition of the metal complexes **(3, 7).**

Complexes.Compd. No.	Decomp. Temperature (°C)	Tp/K	ΔE^* (K J mol^{-1})		R^2		A (S^{-1})		ΔS^* (J K^{-1} mol^{-1})		ΔH^* (K J mol^{-1})		ΔG^* (K J mol^{-1})	
			CR	HM	CR	HM	CR	HM	CR	HM	CR	HM	CR	HM
(3)$[(CuCl_2)_2(HL)(H_2O)_4].H_2O$	438-510	465	343.58	352.79	0.085	0.885	$9.3x10^{38}$	$8.2x10^{39}$	497.45	515.58	339.71	348.92	108.34	109.12
	510-605	565	181.76	51.32	0.992	0.993	$4.8x10^{16}$	$1.1x10^{9}$	74.57	72.07	179.32	48.88	157.5	69.97
	605-923	858	665.52	314.8	0.82	0.83	$3.9x10^{40}$	$1.3x10^{28}$	528.78	287.99	660.65	30.99	352.19	141.31
(7)$[(UO_2)_2(HL)(NO_3)_4].H_2O$	301-32	319	368.28	381.79	0.97	0.96	$4.7x10^{6}$	$1.3x10^{63}$	916.13	963.06	365.63	379.14	73.14	71.66
	324-457	451	602.21	95.62	0.93	0.94	$8.1x10^{69}$	$3.8x10^{28}$	109.79	306.50	600.73	94.14	405.03	39.49

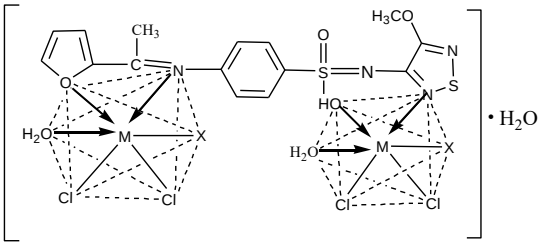

M = Fe(III) , X = Cl
M = Cu(II) , X = H2O
M = Zn(II) , X = H2O
M = Cd(II) , X = H2O
M = Ce(III) , X = H2O

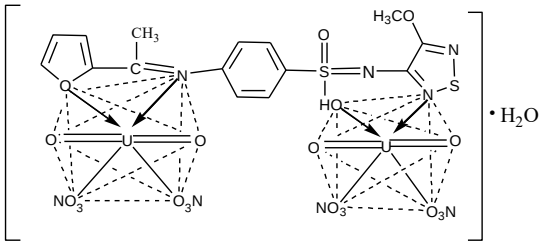

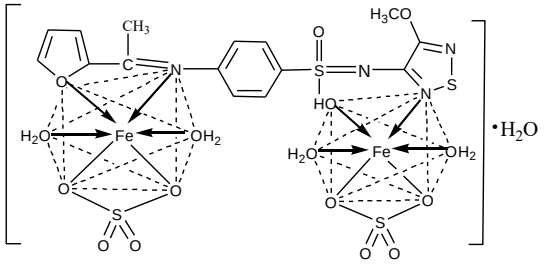

Fig.4. The suggested structures of the newly metal complexes.

3.8.Transmission electron microscopy (TEM)

Transmission electron microscopy (TEM) is used to describe the size and shape of all nano-sized samples copper and zinc nanoparticles of HL Schiff base ligand **Figs. 5, 6.**

The size and morphology of copper and zinc nanoparticles (CuNPs, ZnNPs) with HL Schiff base ligand were investigated by TEM (Transmission electron microscopy) as show in **Figs. 5, 6.** The TEM images indicate that the copper and zinc nanoparticals show spherical shape with core shells of the Schiff-base ligands[49].

The TEM images further revealed the stabilization of copper and zinc nanoparticles due to interaction with the (HL) ligand. This stabilization facilitates penetration of tumor cell membrane and cause the destruction of tumor cell by CuNPs and ZnNPs[50,51]. The CuNPs and ZnNPs sizes are of 50, 60 nm respectively.

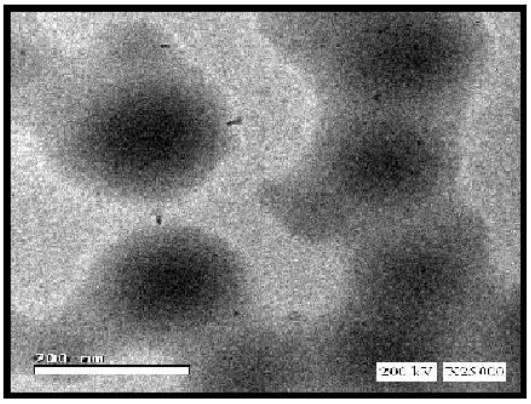

Fig. 5.TEM of CuNps with HL Schiff base ligand **.**

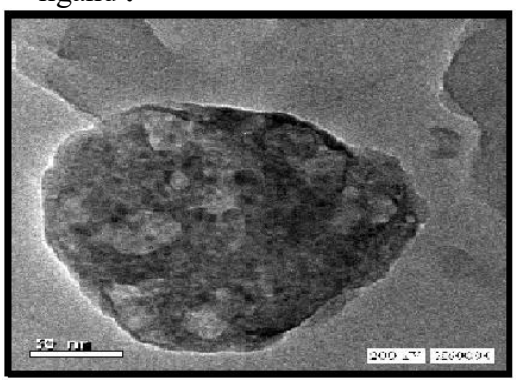

Fig. 6.TEM of ZnNps with HL Schiff-base ligand **.**

3.9. Antimicrobial activity

The main aim of the production and synthesis of any antimicrobial compound is to inhibit the causal microbe without any side effects on the patients[53].

The antimicrobial activity of the parent Schiff base ligand HL and its metal complexes, copper and zinc nano particle size (CuNps,ZnNps) against micro-organism, Gram positive(+ve) bacteria; *Staphylo-coccus aureus (ATCC 25923) and Bacillus subtilis (ATCC 6635)*, Gram negative (-ve) bacteria *Salmonella typhim-urium (ATCC 14028)* and *Escherichia coli (ATCC 25922)*, yeast; *Candida albicans (ATCC 10231)* and fungi; *Aspergillus fumigatus* was tested in order to assess their potential antimicrobial agents.

The biological activity of the Schiff base ligand HL and its metal complexes (1-7), copper and zinc nano particle size (CuNps,ZnNps) were also compared with Chloramphenicol and Cephalothin which were used as standard antibacterial control and Cyloheximide as standard yeasts and fungi control . The data are listed in **Tables 8,9** and **Figs.7-12.** According to the data it can be seen that the HL Schiff base ligand show approximately high activity towards Gram (+ve), Gram(-ve) strains of bacteria and towards Yeasts and Fungi, while all the complexes showed high activity towards Gram positive(+ve) bacteria; *Staphylo-coccus aureus (ATCC 25923)* and *Bacillus subtilis (ATCC 6635)*, Gram negative (-ve) bacteria *Salmonella typhimurium (ATCC14028)* and *Escherichia coli (ATCC 25922).*

The orders of the activity of the metal complexes of HL Schiff base ligand was as follows:

In case of *Staphylococcus aureus* (ATCC 25923):

Ce (III)> Fe(II)> Cd(II)> Fe(III) >UO_2(II) >Zn(II).

In case of *Bacillus subtilis(ATCC6635)*:

Cd(II)>Ce(III)>UO_2(II)>Fe(III)>Cu(II)> Fe(II)>Zn(II).

In case *Salmonella typhimurium(ATCC-14028)*:

Ce(III) >Cd(II) > Fe(II) > Zn(II) >Fe(III).

In case of *Escherichia coli(ATCC 25922)*:

Cd(II) >Fe(III) >Zn(II) >UO_2(II) > Fe(II) > Cu(II) > Ce(III).

On the other hand, all metal complexes (1-7) have intermediate activity towards Yeast; *Candida albicans (ATCC 10231)* and Fungi; *Aspergillus fumigatus*.

The orders of the activity of the metal complexes was as follows:

In case of *Candidaalbicans*(ATCC10231):

Cd(II)>Cu(II)>UO_2(II)>Fe(III)>Zn(II)> Fe(II)>Ce(III).

In case of *Aspergillus fumigatus*:

Fe(III) > Cd(II) >Cu(II) > Ce(III) > UO_2(II).

The copper nanocompoite (CuNps) records high activity towards Gram positive(+ve) bacteria; *Staphylococcus aureus (ATCC 25923)* and *Bacillus subtilis (ATCC 6635)*, Gram negative (-ve) bacteria *Salmonella typhimurium (ATCC 14028)* and Escherichia coli *(ATCC 25922)*, Yeast; *Candida albicans (ATCC 10231)* and Fungi; *Aspergillus fumigatus*. Although zinc nanocomposite (ZnNps) reveals intermediate activity towards Gram positive(+ve) bacteria, while its discourage the activity of its parent HL Schiff base ligand,Gram negative (-ve) bacteria, Yeast and Fungi.

So the order of the activity of the metal complexes was as follows:

In case of *Staphylococcus aureus (ATCC 25923)*:

CuNps>ZnNps>HL>Zn(II)complex.

In case of *Bacillus subtilis(ATCC 6635)*:

CuNps>HL>ZnNps>Cu(II)complex> Zn(II)complex.

In case of *Salmonella typhimurium (ATCC 14028):*

CuNps>Zn(II)complex>ZnNps=Cu(II) complex = HL.

In case of *Candida albicans(ATCC 10231):*

CuNps>Zn(II)complex> Cu(II)complex= HL>ZnNps(NA).

In case of *Aspergillus fumigatus*:

CuNps>HL>Cu(II)complex>Zn(II)complx (NA)=ZnNps(NA).

Table 8. Antimicrobial activity of HL Schiff base ligand and its complexes **(1-7).**

	Zone diameter (mm). Microorganisms.											
	Gram - positive bacteria				**Gram - negative bacteria**				**Yeasts and Fungi**			
	Staphylococcus aureus(ATCC 25923)		*Bacillus subtilis* (ATCC 6635)		*Salmonella typhimurium* (ATCC 14028)		*Escherichia coli (ATCC 25922)*		*Candida albicans(ATCC 10231)*		*Aspergillus fumigatus*	
Sample \ Concentration	1 mg/ml	0.5 mg/ml	1 mg/ml	0.5 mg/ml	1 mg/ml	0.5 mg/ml	1 mg/ml	0.5 mg/ml	1 mg/ml	0.5 mg/ml	1 mg/ml	0.5 mg/ml
HL	28H	17I	23I	20H	NA	NA	11I	9I	18I	13I	22I	17I
(1)$[(FeCl_3)_2(HL)(H_2O)_2]\cdot H_2O$	28H	10L	19I	14I	10L	25H	16I	22H	20I	18I	28H	15I
2)$[(FeSO_4)_2(HL)(H_2O)_4]\cdot H_2O$	28H	22H	18I	11I	18I	14I	11L	8L	15I	10I	NA	NA
(3)$[(CuCl_2)_2(HL)(H_2O)_4]\cdot H_2O$	NA	NA	19I	15I	NA	NA	2L	10L	32H	27H	20L	12I
(4)$[(ZnCl_2)_2(HL)(H_2O)_4]\cdot H_2O$	23H	19H	5L	20H	14I	11I	16I	12I	17I	13I	NA	NA
(5)$[(CdCl_2)_2(HL)(H_2O)_4]\cdot H_2O$	28H	21H	32H	29H	19I	17I	21I	17I	35H	24H	22I	19I
(6)$[(CeCl_3)_2(HL)(H_2O)_2]\cdot H_2O$	30H	26H	24H	16I	28H	20H	10L	8L	12I	10I	16I	13I
(7) $(UO_2)_2(HL)(NO_3)_4\cdot H_2O$	26H	18I	19I	16I	NA	NA	14L	11I	25H	20H	17I	8L
Control #	**35**	**26**	**35**	**25**	**36**	**28**	**38**	**27**	**35**	**28**	**37**	**26**

NA= No activity; L: Low activity; I: Intermediate activity; H: High activity.
#: *Chloramphencol* in the case of Gram-positive bacteria, *Cephalothin* in the case of Gram-negative bacteria and *cycloheximide* in the case of Yeasts and Fungi.

Table. 9. Antimicrobial activity of HL Schiff base ligand, its complexes **(3, 4)** and nanocompsite(CuNps,ZnNps) **(1, 2).**

	Zone diameter (mm). Microorganisms.											
	Gram - positive bacteria				**Gram - negative bacteria**				**Yeasts and Fungi**			
	Staphylococcus aureus (ATCC 25923)		*Bacillus subtilis* (ATCC 6635)		*Salmonella typhimurium* (ATCC 14028)		*Escherichia coli (ATCC 25922)*		*Candida albicans (ATCC 10231)*		*Aspergillus fumigatus*	
Sample \ Concentration	1 mg/ml	0.5 mg/ml	1 mg/ml	0.5 mg/ml	1 mg/ml	0.5 mg/ml	1 mg/ml	0.5 mg/ml	1 mg/ml	0.5 mg/ml	1 mg/ml	0.5 mg/ml
HL	28H	17I	23I	20H	NA	NA	11I	9I	18I	13I	22I	18I
(3)$[(CuCl_2)_2(HL)(H_2O)_4]\cdot H_2O$	NA	NA	19I	15I	NA	NA	10L	10L	32H	27H	20L	12I
(1) Cu Nps	31H	22H	38H	29H	29H	30H	28H	10L	32H	17I	30H	23H
(4)$[(ZnCl_2)_2(HL)(H_2O)_4]\cdot H_2O$	23H	19H	5L	20H	14I	11I	16I	12I	17I	13I	NA	NA
(2) ZnNps	27H	20H	20I	15I	NA	NA	NA	NA	NA	NA	NA	NA
Control #	**35**	**26**	**35**	**25**	**36**	**28**	**38**	**27**	**35**	**28**	**37**	**26**

NA= No activity; L: Low activity; I: Intermediate activity; H: High activity.
#: *Chloramphencol* in the case of Gram-positive bacteria, *Cephalothin* in the case of Gram-negative bacteria and *cycloheximide* in the case of Yeasts and Fungi.

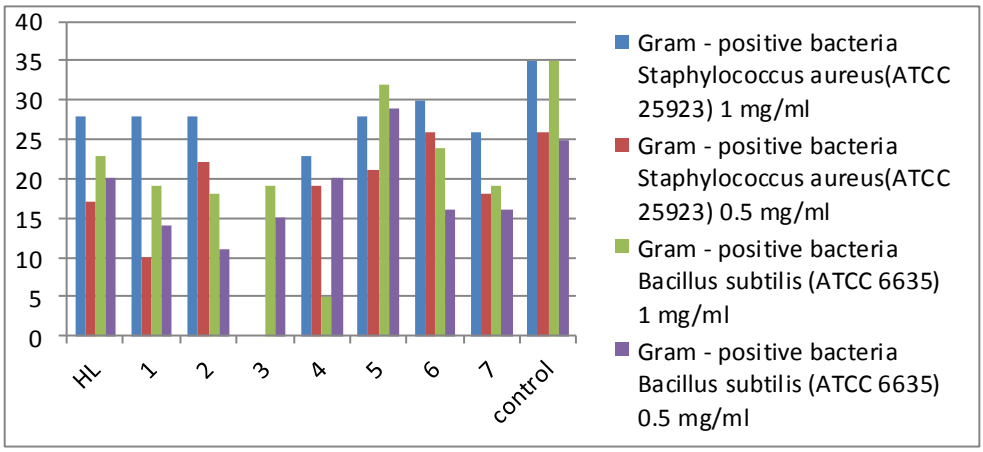

Fig. 7. Antibacterial activity of HL Schiff base ligand and its metal complexes**(1-7)** against Gram (+ve) bacteria

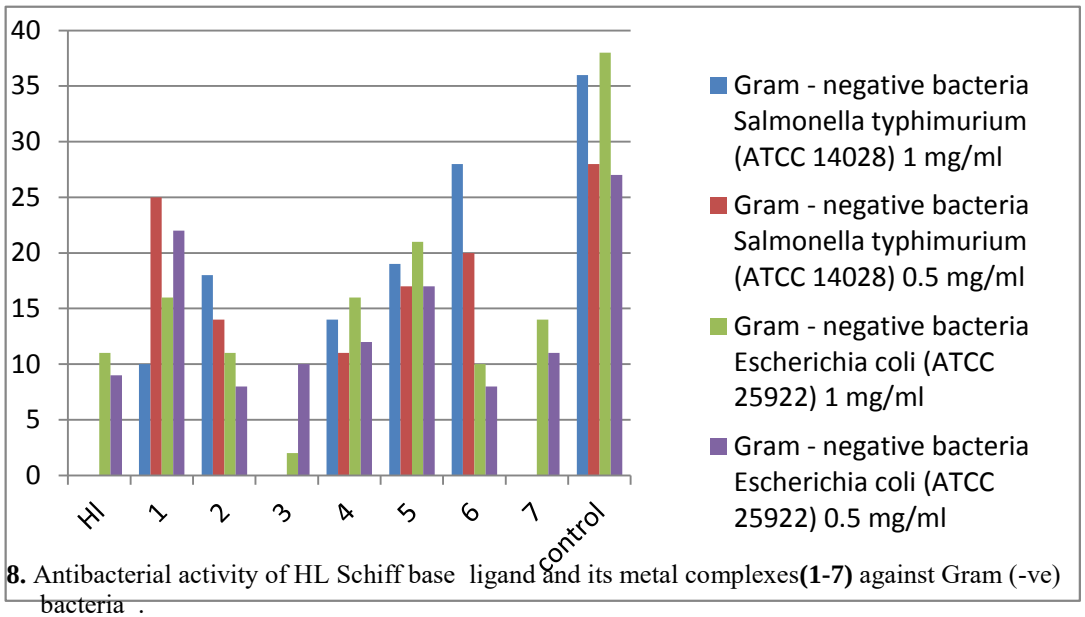

Fig. 8. Antibacterial activity of HL Schiff base ligand and its metal complexes**(1-7)** against Gram (-ve) bacteria .

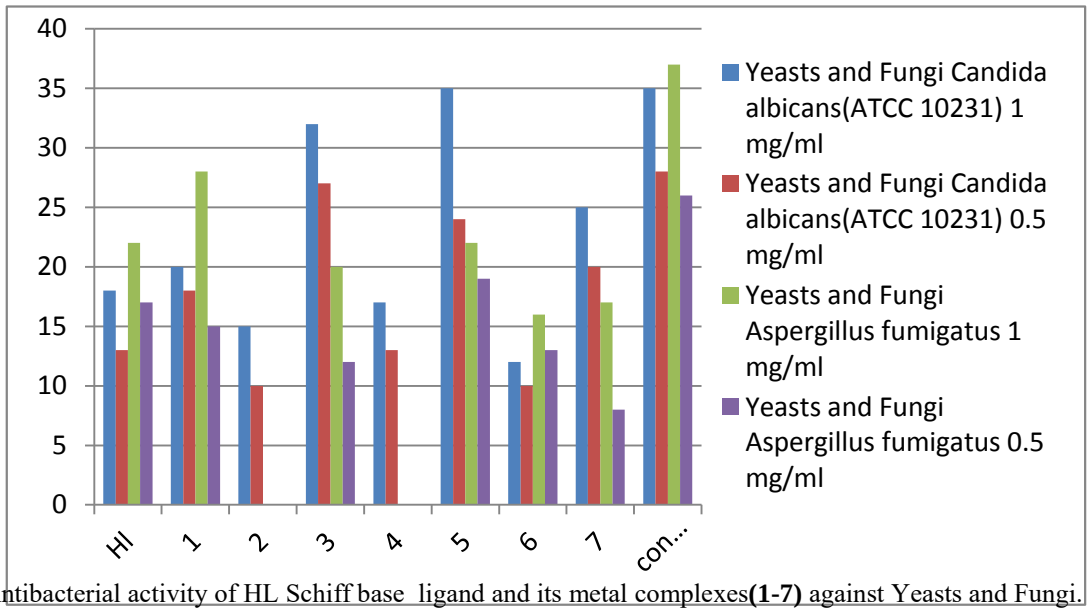

Fig.9. Antibacterial activity of HL Schiff base ligand and its metal complexes**(1-7)** against Yeasts and Fungi.

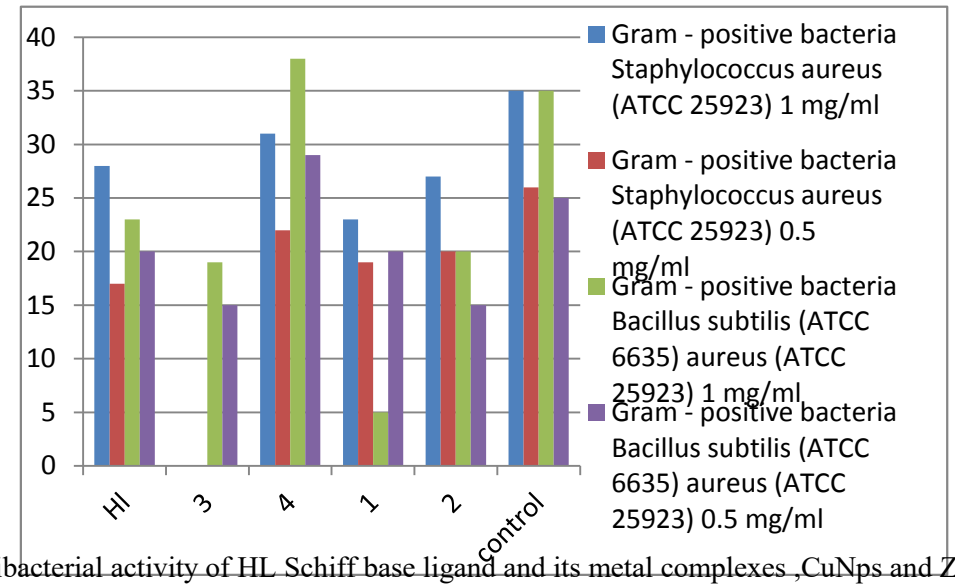

Fig. 9. Antibacterial activity of HL Schiff base ligand and its metal complexes ,CuNps and ZnNps **(3,4, 1, 2)** against Gram (+ve) bacteria**.**

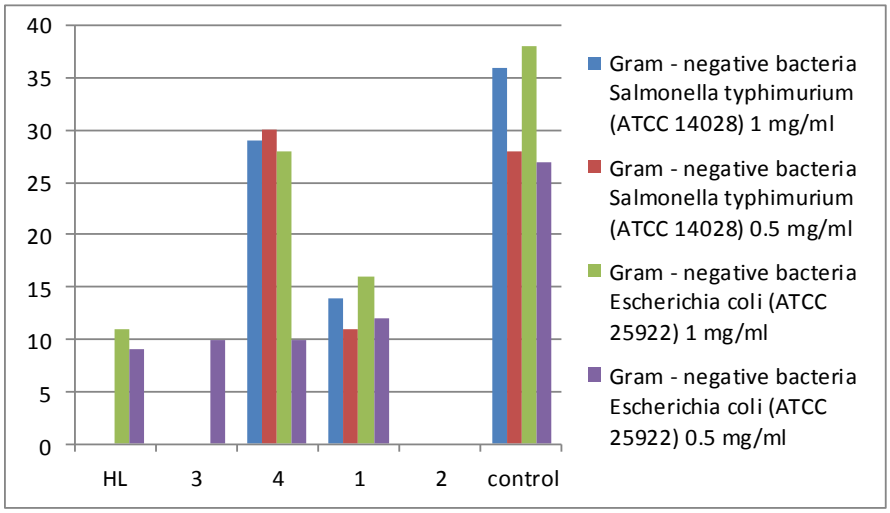

Fig . 11. Antibacterial activity of HL Schiff base ligand and its metal complexes, CuNps and ZnNps**(3, 4 , 1, 2)** against Gram (-ve) bacteria .

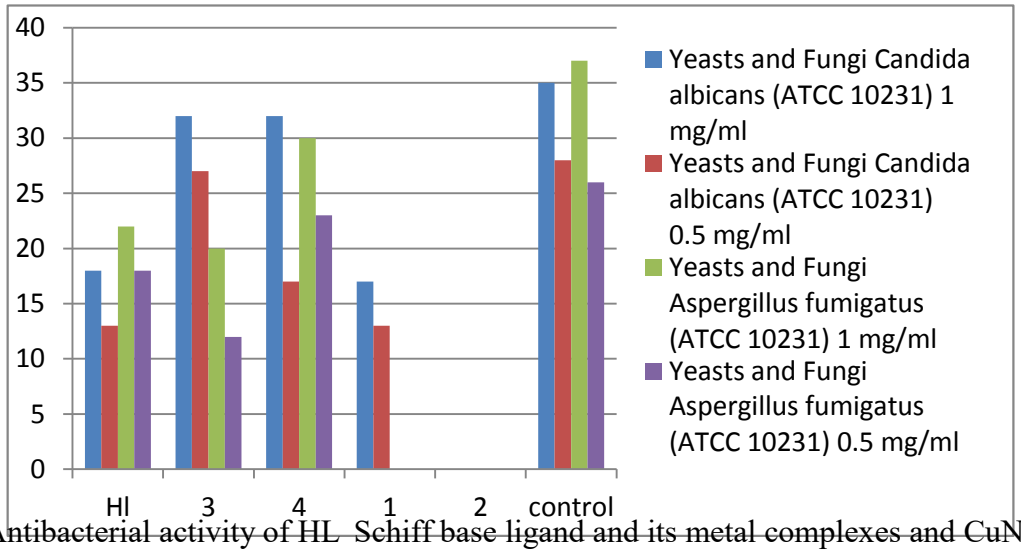

Fig .12. Antibacterial activity of HL Schiff base ligand and its metal complexes and CuNps and ZnNps **(3, 4 , 1,2)** against yeasts and fungi.

3.10 . In-vitro cytotoxicity assays. Evaluation of new synesized ligands and their metal complexes in cancer therapy.

In this study in vitro anticancer activity evaluation of the newly synthesized compounds HL Schiff base ligand and its metal complexes and copper, zinc nano-composites (CuNps,ZnNps) was carried out against human cancer cell line (HCT-116) (human colon cancer cell liens) also, called colorectal cancer or bowel cancer, which is the third most common form of cancer[54].The relationship between drug concentrations and cell viability was plotted to calculate IC_{50} (µg)(the value which corresponds to the concentration required for 50% inhibition cell viability) and the data were presented in **Table 11**. Almost all tested compounds are effective against HCT-116 (Colon cancer). The data illustrate that:

The HL Schiff base ligand inhibition against HCT-116 cell line records 59.69%, while its copper and zinc nanocomposite (CuNps,ZnNps)records the highest inhibition equal to 93.96%.

Also the IC_{50} values for HL Schiff base ligand, its complexes and nanoconposites were presented in **Table 11** .The data shows that the copper nanocomposit (CuNps) have the highest IC_{50} value equal to 2.60µg against colon carcinoma cell line HCT-116, while its HL Schiff base ligand records IC_{50} equal to 32.42µg.

The data records that the order of the anticancer activities is:

CuNps = $[(CuCl_2)_2$ (HL) $(H_2O)_4].H_2O$ > ZnNps >$[(CeCl_3)_2$ (HL)$(H_2O)_2].H_2O$ > $[(ZnCl_2)_2(HL)(H_2O)_4]$. H_2O>HL >$[(UO_2)_2$ (HL)$(NO_3)_4].H_2O$.

Tabel 10. Antitumor activity of HL ligand Cu(II), Zn(II), Ce(III) andUO_2(II) complexes, CuNps and ZnNps**.**

HCT-116	
Samples	**Inhibition%**
HL	59.69
(3)$[(CuCl_2)_2(HL)(H_2O)_4]\cdot H_2O$	89.81
(4)$[(ZnCl_2)_2(HL)(H_2O)_4]\cdot H_2O$	80.81
(6)$[(CeCl_3)_2(HL)(H_2O)_2]\cdot H_2O$	84.25
(7) $[(UO_2)_2(HL)(NO_3)_4]\cdot H_2O$	31.82
(1) Cu Nps	93.96
(2) Zn Nps	91.38

Tabel 11. Inhibition of cell proliferation (IC_{50}µg) for HL free ligand, its metal complexes and nanocomposites(CuNps, ZnNps).

HCT-116	
Samples	**IC_{50}(µg)**
HL	32.42
(3)$[(CuCl_2)_2(HL)(H_2O)_4]\cdot H_2O$	5.81
(4)$[(ZnCl_2)_2(HL)(H_2O)_4]\cdot H_2O$	19.23
(6)$[(CeCl_3)_2(HL)(H_2O)_2]\cdot H_2O$	10.32
(7) $[(UO_2)_2(HL)(NO_3)_4]\cdot H_2O$	50
(1) Cu Nps	2.60
(2) Zn Nps	8.94

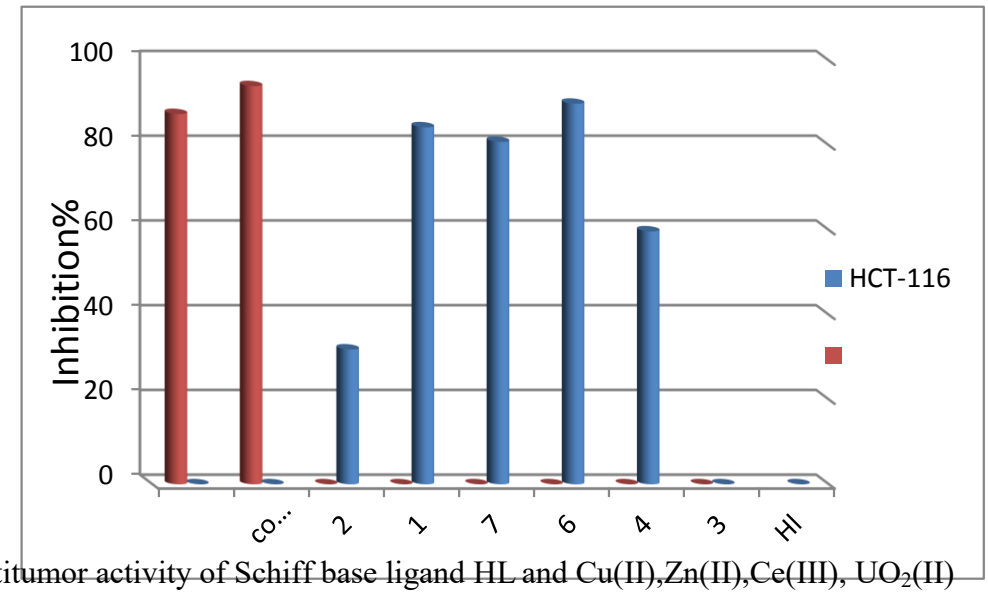

Fig.13. Antitumor activity of Schiff base ligand HL and Cu(II),Zn(II),Ce(III), UO_2(II) complexes, CuNps and ZnNps.

References

1- Z. Hussain, E. Yousif and A. Altaie, Organic and medicinal Chemistry letters.,**4**, 1 (2014).

2- A.S. Abu-Khadra, R.S. Farag and A. E.M. Abdel-Hady, Ame. Journal of Analytical Chemistry, **7**,233-245(2016).

3- H.A.Bayoumi, A.M.A.Alaghaz and M.S.Aljahdali, Int. J. Electro Chem. Sci.,**8**, 9399-9413(2013).

4- S.K.Hadjikakou and N.Hdjiliadis, Coord. Chem. Rev.,**253**, 235-249 (2009).

5- A.Shokrollahi,M.Ghaedi,N.Khanjari, S. Noshadi and S. Joybar, E-Journal Chemistry,**8(2)**, 495-506(2011).

6- O.Kocyigit and E.Gulcur, J.Incl. Phenom.Macrocyle.Chem., **67**,287-293(2010).

7- E.Ispir,Dyes and Pigments,**82**,13-19 (2009) .

8- V.L.Siji, M.R.Sudarsanakumar and S.Suma, Transition Metal Chemistry, **36**, 417-424(2011).

9- S.Eswaran, A.V.AdhiKari and N.S. Shetty, Eur. Journal of Medicinal Chemistry,**44**, 4637-4647(2009).

10- P.H.C.Camargo,K.G.Satyanarayana and F.Wypych, Materials Research, **12**, 1-39(2009).

11- A.R. Ibrahim, Int. J. Adv. Res., **3(8)**, 315- 324 (2015).

12- A.A. El-Sherif and T.M.A. Eldebss, Spectro Chim. Acta A, **97**,1803-1814 (2011).

13- M.S. Refat, F.M. AlAzab, H.M. A. Al-Maydama, R.R. Amin and Y. M. S. Jamil, Journal of Molecular Structure, **1059**, 208 224 (2014).

14- A. Saxena, Adv. Appl. Sci. Res., **4 (4)**, 152-154 (2013).

15- I.P. Ejidike and P.A. Ajibade, Int. J. Mol. Sci., **17**,60(2016).

16- A. Athar, F. Khan, W. Ahmed, Z. Hag and Z. Khan, Amer. Eur. J.Agric and Environ. Sci.,**15(1)**,36-67(2015).

17- D.P. Patel, S.P. Prajapati, A.K. Rana and P.S. Patel, Der Chemical sinca., **3 (2)**,491-496 (2012).

18- G.G. Mohamed, M.A. Zayed and S.M. Abdallah, J. Molec. Struc., **979**,62-71(2010).

19- A.A. Alomari, J.Atoms and Molecules, **4(2)**, 693-704(2014).

20- M.E.Azab, S.A. Rizk and A.E.-G. Amr, Molecules, **20**, 18201-18218 (2015).

21- A.-N. M.A. Alaghaz, H. A. Bayoumi, Y. A. Ammar and S. A. Aldhlmani, J. Mol. Struct., **1035**, 383-399(2013).

22- H. A. Bayoummi,A-N. M.A. Alaghaz, and M. S. Aljahdali, Int. J. Electrochem. Sci., **8**, 9399-9413(2013).

23- B. Jain, S.Malik, N.Sharma and S. Sharma, Der Chemica Sinica., **4(5)**,40-45(2013).

24- A. Jebali, F. Ramezani and B. Kazemi, J. Clust. Sci., **22**, 225–232 (2011).

25- G.G. Mohamed, M.M.Omar, and A.M. Hindy, Turk., J. Chem., **30**, 361−382 (2006).

26- G.G. Mohamed, Phosphrous Sulfur Silicon Related Elements, **180 (7)**, 1569(2005).

27- M. Asadi, M.S.Khah and A.H.Kianfar, J. Irna. Chem. Soc.,**7(1)**, 38-44(2010).

28- M.S. Balakrishna, D. Suresh, A . Rai, J.T. Mague and D. panda, Inorg. Chem., **49**,8790-8801(2010).

29- G.G. Mohamed and C.M. Sharaby, Spectro Chim. Acta, Part A, **66**, 949 (2007).

30- C.M.Sharaby, Synth. and React. Inorg. Met. Org. and Nano-Met. Chem., **35**, 133–142(2005).

31- K.Vimala, K. S. Sivudu,Y. M.Mohan, B.Sreedhar and K.M.Raju, Carbohydrate Polymers, **75**, 463–471 (2009).

32- A.M.A. Alaghaz and R.A.Ammar,Eur. J.Med.Chem.,**45**,1314-1322 (2010).

33- A.Jain and S.Valecha, Acta Chim. Phrm. Indica., **5(2)**,55-59 (2015).

34- S. Sharma,N. Sharma, B. Jain and S. Malik, Der chemica Sinica., **5(5)**,61-66(2014).

35- N. Nawar, I.I. El-Swwah, N.M. Hosny M. M. Mostafa, phosphorous, Sulfur and Silicon and related elements, **187**,976(2012).

36- U. k. Singh, S.N. Pandeya, S. K. Sethia, M. Pandey, A. Singh, A. Garg and P. Kumar. Int. J.Phamaceutical Sciences and Drug Research, **2(3)**, 216-218(2010).

37- A.A. Abdel Aziz, A.M. Salem, M.A. Sayed, and M.M. Aboaly, J. Mol. Struct., **1010**, 130–138(2010).

38- A.M.A. Alaghez, B.A. El-Sayed and R.A.A. Ammar, Mol . Struct., **1035**, 83-93(2013).

39- V.R.Solomon,C. Hua and H.Lec, Bioorg. Med. chem., **17**, 7585(2009).

40- M. F. Hochella J. Nanoscience and technology, **203**, 593-605 (2002).

41- G. G.Mohamed,N.E.A.El-Gamel and F. A. N.El-Dien, Synth. React. Inorg. Met. Org. Chem., **31(2)**, 347(2001).

42- E. Yousif, Lambert Academic, Saabrucken, (2012).

43- G.G.Mohamed, Phosphrous Sulfur Sinlicon related Elements ,**180(7)** , 1569 (2005).

44- M.Odabasoglu, S.Cakmak, G.Turgut, and H. Icbudak, Phsphrous, Sulfur and Silicon, **178**,549-558(2003).

45- K.Mohanan,C. J. Athira,Y. Sindhu and M.S. Sujamol,J. Rare Earths, **27(5)**, 705(2009).

46- W.H. Hegazy and I. H .Al-Motowaa, Bioinrg. Chem. Appls., 1,201(2011).

47- E. Kremer, G. Facchin, E. Estevez, P. Albores, E.J. Baran, J. Ellena and M.H. Torre, J. Inorg. Biochem, **100**, 1167–1175 (2006).

48- S.S.Stokes, R.Albert, E. T.Buurman , Andrews B., A. B.Shapiro, O. M. Green, A.R.McKenzie and L.R. Otterbein, Bioorg and Med. Chem. Lett., **22**, 7019 (2012).

49- N. Ozbek, H. Katircioglu, N. Karacan and T. Baykal, Bioorg. Med. Chem., **15**, 5105–5109(2007).

50- M.Asadi, M.S. Khah and A.H.Kianfar, J.Iran .Chem. Soc., **7(1)**, 38-44 (2010).

51- G .E. Amer, Ph.D. Thesis, Faculty of Science, Ain–Shames University, Cairo, Egypt (2011).

52- G.M.S.Elsharfei, F.Z. Yehia, O.I.H. Dimitry, A.M.Badwi and G. Eshaq, Applied Catalysis B: Enviromental, **99**,242-247(2010).

53- M.M.H.Khalil, E.H.Ismail, G.G. Mohamed, E.M.Zayed and A.Bader, J. Inorg. Chem.,**2**,13-21(2012).

45- P.Skehan, R .Strreng and D. Scudiero, J .Nati . Cancer Inst., **82(13),** 1107-112(1990).